Localized surface plasmon modes of core–shell bimetal nanowires do not hybridize

Elena A. Velichko

Department of Quantum Electronics and Nonlinear Optics, O. Y. Usikov Institute of Radio-Physics and Electronics NASU, Kharkiv 61085, Ukraine
(elena.vel80@gmail.com)

We investigate localized plasmon-mode resonances in the scattering and absorption of transversely polarized light by bimetal core–shell nanowires made of silver and gold, in two possible combinations, using an analytical solution and experimental data for metal permittivities. In particular, the influence of the metal shell thickness and material on these resonances is studied. We show that, unlike metal nanotubes with dielectric filling, bimetal wires do not display plasmon-mode hybridization.   © 2020 Optical Society of America

https://doi.org/10.1364/JOSAA.397200

1. INTRODUCTION

Bimetallic nanowires are explored today for applications in, among others, surface-enhanced Raman scattering sensors [1] and flexible electronics [2]. This is because solid noble-metal nanoparticles and nanoshells are known to behave as resonant scatterers of light in the visible range, due to the localized surface plasmon (LSP) modes [3–6]. Their resonance wavelengths depend on the type of metal and, for nanoshells, vary strongly with the shell thickness. It is interesting to see how LSP-mode resonances appear on a bimetal core–shell nanowire. In [7], such resonances were investigated for a circular bimetal wire using a one-term quasi-static approximation and analytical Drude formulas for the silver and gold dielectric functions. This analysis appears too rough and, for any practical use, should be replaced with full-wave electromagnetic engineering. We consider the scattering of light from bimetal silver–gold and gold–silver nanowires, where the first metal is the material of the core and the second is that of the shell. Unlike [7], our numerical results are based on the full-wave analytical solution, in the form of the series in the azimuthal Fourier orders. This solution uses the separation of variables in the polar coordinates. It was invented by Lord Rayleigh in 1881 [8] and can also be found in [4,6,9–11]; sometimes, in error, it is referred to as "Mie theory." In addition, we use experimental data for the refractive index of gold and silver from [12] because, unlike the Drude formula, they are accurate in the violet range. These data are combined with a smoothing algorithm based on the Akima spline interpolation, to yield continuous functions.

We present the spectral and spatial characterization of LSP resonances in the silver–gold and gold–silver bimetallic nanowires as a function of their geometrical parameters. For better insight into the LSP mode properties of bimetal wires, we compare them with more frequently studied hybrid LSP modes of metal nanotubes of the same size and thickness. As the LSP modes are the boundary states, the presence of two metal–dielectric boundaries in nanotubes leads to strong coupling and, hence, hybridization of the "inner" and "outer" LSP modes of the same azimuthal index, controlled by the tube thickness. We show that bimetal wires, of either composition, do not show such hybridization as they have only one, outer, boundary between the metal and the dielectric. If the shell is sizably thicker than the skin depth, then the LSP resonance in the scattering and absorption is one and associated with the metal and outer radius of the shell. However, if the shell gets thinner than the mentioned depth, then the core starts shining through it at the wavelength, determined by the metal and radius of the core.

2. SCATTERING PROBLEM

We consider the H-polarized plane wave incident normally on a circular bimetal wire placed in vacuum; see Fig. 1. The inner radius of the scattering structure, i.e., the core, is a and the outer radius is $b = a + h$, h being the thickness of the shell. We introduce cylindrical coordinates, co-axial with the wire. The method of separation of variables enables us to derive an analytical solution, the details of which can be found in many sources, for instance, in [6,8–11] for the two-layer core–shell circular wire with arbitrary dielectric permittivities. To generate the numerical results, we use Eqs. (2)–(10) of [6], where the series are truncated to the finite order of such a value, which guarantees five or more correct digits.

3. NUMERICAL RESULTS

Based on the full-wave analytical series solution, we have computed the total scattering cross section (TSCS) and the
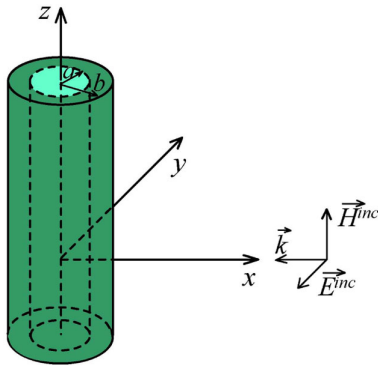
Fig. 1.   Geometry of bimetal nanowire placed into free space.

absorption cross section (ACS) of the studied bimetal nanowires as a function of the wavelength and other parameters.

To have a reference, at first we present in Figs. 2 and 3 the spectra of the TSCS and ACS in the ultraviolet and visible ranges, for silver and gold nanotubes in vacuum, respectively, with inner void radius $a = 20$ nm and several values of shell thickness, h. They show peaks at the wavelengths of hybrid LSP modes, studied in [5,6]. These wavelengths are different for different m and strongly depend on the shell thickness. In Fig. 2, one can see that making this value smaller shifts the wavelengths of the LSP modes of the "difference" family, P_1^-, P_2^-, ..., to

the red and the other, "sum" family, P_1^+, P_2^+, ..., to the blue. Conversely, making the tube thickness greater than the skin depth (that is around 15 nm) brings these wavelengths together at the wavelength of approximately 337 nm for silver.

It is useful to note that, on a solid metal nanowire of radius a the LSP modes, P_m, are found in all azimuth indices, $m \geq 1$. However, their wavelengths do not depend, in the main term, on m and satisfy the quasi-static equation (see, e.g., [3], p. 431),

$$\mathrm{Re}\,\varepsilon_M(\lambda_m) = -1 + O(a^2/m\lambda^2). \tag{1}$$

Together with the data of [12] for $\varepsilon_M(\lambda_m)$, Eq. (1) yields $\lambda_m = 339$ nm for silver. Thus, all LSP modes cluster near the same wavelength. Therefore, as the silver is sizably lossy, the corresponding to them resonance peaks merge together.

Unlike the silver nanotube, similar plots for the gold nanotube (Fig. 3) demonstrate only one well visible peak. It can be identified as the resonance on the hybrid LSP mode P_1^- while that on the sister mode P_1^+ is not visible because of the large bulk losses in gold in the violet and ultraviolet ranges (around 6 times larger than the silver according to [12]).

Moreover, if the tube thickness gets larger, then the LSP peak tends not to the root of Eq. (1) that is, according to [12], $\lambda = 234$ nm, but to approximately 500 nm. Careful inspection shows that Eq. (1) follows from more general equation, $\varepsilon_M(\lambda_m) = -1$, if the losses in the metal are neglected. This is
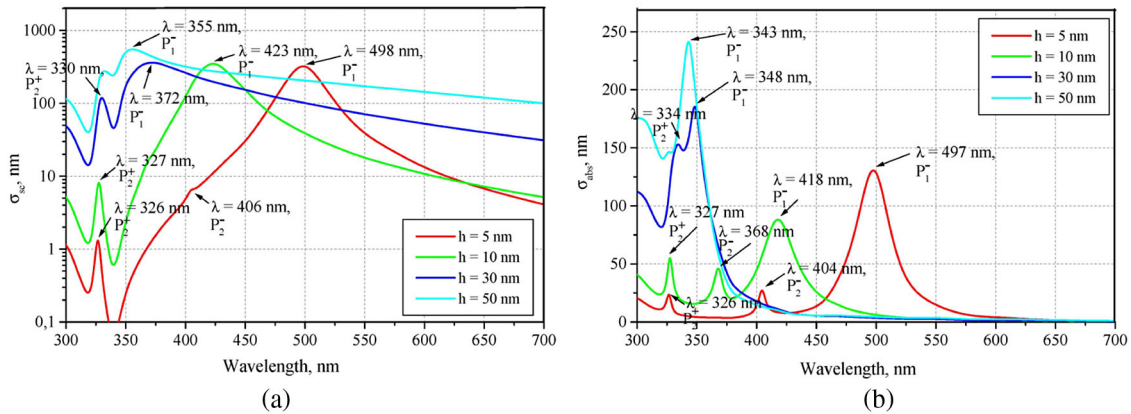
Fig. 2.   Spectra of (a) TSCS and (b) ACS for the silver tube in air, for several values of tube thickness. The inner radius of tube $a = 20$ nm.
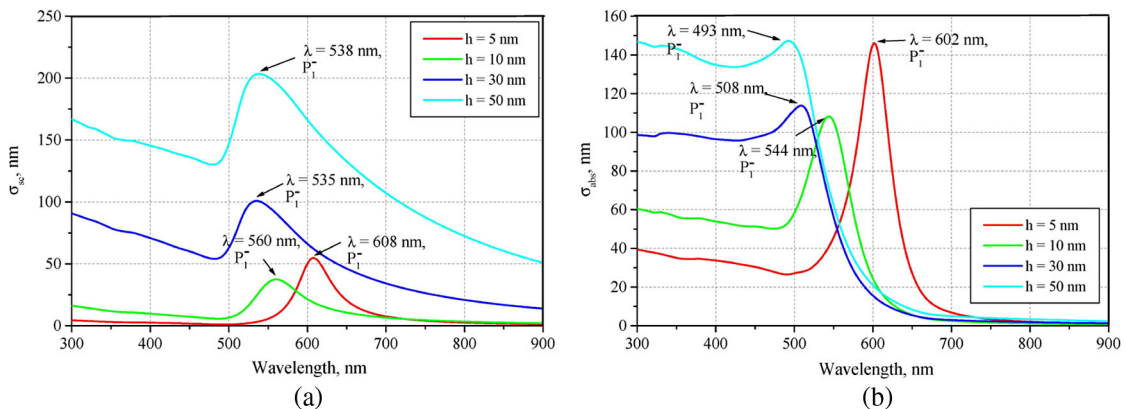
Fig. 3.   Same as in Fig. 2, but for the gold tube in air.

because, if $a/\lambda << 1$, each term in the Fourier-series analytical solution obtains the expression $\varepsilon_M + 1$ in the denominator.

Therefore, if a metal such as gold has sizable losses, Eq. (1) is inaccurate and should be replaced with the equation for the minimum of the function $|\varepsilon_M(\lambda) + 1|$. This yields

$$\mathrm{Re}\varepsilon_M(\lambda_m) = -1 - \mathrm{Im}\varepsilon_M(\lambda_m) \left. \frac{d\,\mathrm{Im}\varepsilon_M(\lambda)/d\lambda}{d\,\mathrm{Re}\varepsilon_M(\lambda)/d\lambda} \right|_{\lambda=\lambda_m}$$
$$+ O(a^2/m\lambda^2). \qquad (2)$$

The data of [12] deliver the root of Eq. (2) at $\lambda_m = 512$ nm that is close to the observed value.

Hybridization of the metal nanotube LSP modes, in each azimuth index $m \geq 1$, implies splitting into two families, corresponding to the $P_m^{\pm}$ modes. If the outer medium is air, then the quasi-static equations for their wavelengths are (see [5])

$$\mathrm{Re}\varepsilon_M(\lambda_m^{(\pm)}) = -\frac{(\mathrm{Re}\varepsilon_{in} + 1)}{2}\xi_m$$
$$\pm \left[\frac{(\mathrm{Re}\varepsilon_{in} + 1)^2}{4}\xi_m^2 - \varepsilon_{in} \right]^{1/2} + O(a^2/m\lambda^2), \qquad (3)$$

where $\xi_m = (1 + \gamma^{2m})/(1 - \gamma^{2m})$, $\gamma = a/(a+h)$, $m = 1, 2, \ldots$, and $\varepsilon_{in}(\mathrm{Re}\varepsilon_{in} > 0)$ is the relative dielectric permittivity of the inner filling material. Note that if $h/a \to \infty$, then each of $(\pm)$ equations in Eq. (3) transforms to Eq. (1). Conversely, if $h/a \to 0$, then $\xi_m >> 1$ and the difference between the roots of $(+)$ and $(-)$ equations of Eq. (3) tends to infinity. As visible from Fig. 2, the spectral shift to the red of the peak on the P_1^- mode becomes dramatically large if the shell thickness is in units of nanometers, i.e., smaller than the skin depth in the visible range [5].

This behavior can be understood taking into account that flat interface between a conventional lossless dielectric with permittivity $\varepsilon > 1$ and a noble metal with $\mathrm{Re}\varepsilon_M < 0$ supports surface plasmon wave. The wavenumber or propagation constant of this wave is

$$\gamma_{\mathrm{plas}} = k\left(\frac{\varepsilon_M}{\varepsilon_M + \varepsilon}\right)^{1/2}. \qquad (4)$$
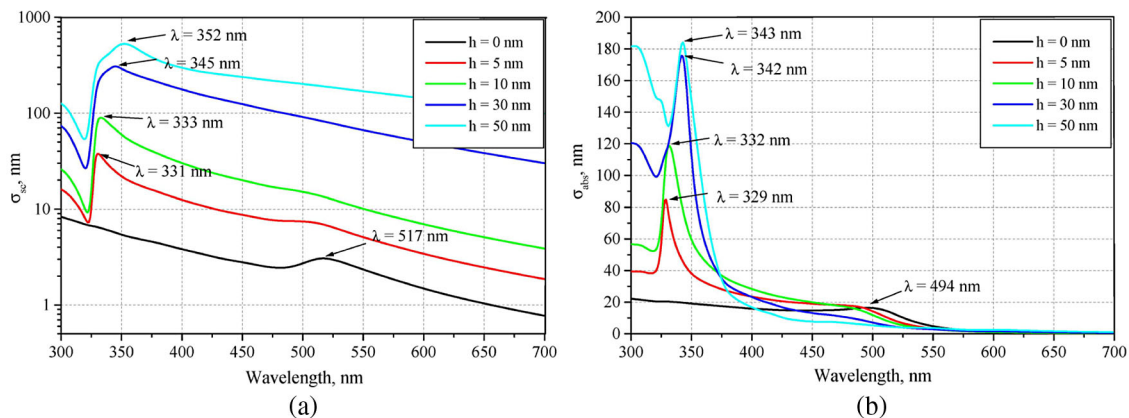
In view of losses in the metal, this is a complex number. It is easy to see that such a wave, as a root of dispersion equation, exists only if $\mathrm{Re}\varepsilon > 0$ and then $\mathrm{Re}\gamma_{\mathrm{plas}} > k$. On the wire boundary, such a wave creates standing waves if the circumference equals to the integer number, m, of surface-wave lengths—these are the LSP modes P_m. For a metal nanotube, such boundaries are two, the inner and the outer, and this leads to the mode hybridization caused by the strong coupling between these modes.

Keeping in mind the results for metal nanotubes in air, we present in Figs. 4 and 5 similar plots for bimetal wires with gold (silver) core and silver (gold) shell, respectively. They demonstrate very different, from nanotube, spectra of the scattering and absorption. If the shell is thicker than the skin depth (around 15 nm), then only one peak is visible in the scattering, at around $\lambda = 343$ nm in Fig. 4(a) and at $\lambda = 517$ nm in Fig. 5(a). This peak is related to the collective LSP resonance of the solid nanowire made of silver or gold, i.e., of the shell material. In the absorption, however, the second peak can be seen. It is very small for the gold core with silver shell, Fig. 4(b); however, it is well visible for the silver core with gold shell, Fig. 5(b).

In sharp contrast to the behavior of the LSP-mode resonances of a noble-metal nanotube in air (see Figs. 2 and 3), making the shell thicker has almost no effect on the resonance (shifts very slightly to the red). Conversely, if the shell becomes thinner than the skin depth (i.e., a few nanometers), then the collective resonance of the LSP modes of the core becomes visible and, in the case of silver core with thin gold shell, even becomes dominant. Its wavelength also is independent of the further thinning of the shell. In the other case (gold core with thin silver shell) the core resonance remains very weak even if the shell is thinner than 5 nm. Such a difference has a clear explanation: silver is considerably less lossy than gold.

All these features, when compared with TSCS and ACS spectra of metal nanotubes in air, demonstrate that the LSP modes of bimetal wires of either core–shell combination do not hybridize. For a better understanding of this behavior, it is useful to recall Eq. (4) once again. Indeed, if the other medium is also a metal, i.e., $\mathrm{Re}\varepsilon < 0$, then formally $\mathrm{Re}\gamma_{\mathrm{plas}} < k$ that means that the surface wave, guided by the boundary between two metals, is absent.

As a result, on the finite-size scatterers like bimetal wire, the LSP modes are associated only with the outer boundary of the

Fig. 4. Spectra of (a) TSCS and (b) ACS for the nanowire with the gold-core radius $a_1 = 20$ nm and varying thicknesses of silver shell.
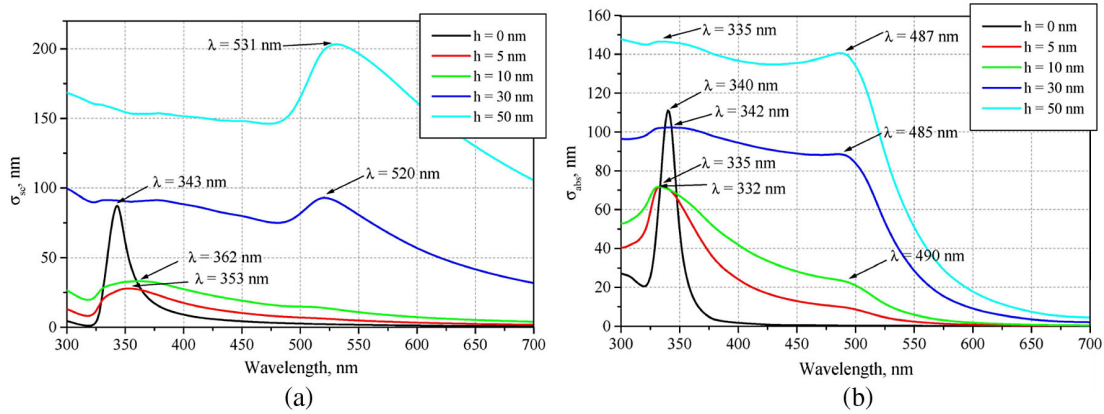
Fig. 5.   Same as in Fig. 4, but for the nanowire with the silver-core radius $a = 20$ nm and varying thicknesses of gold shell.
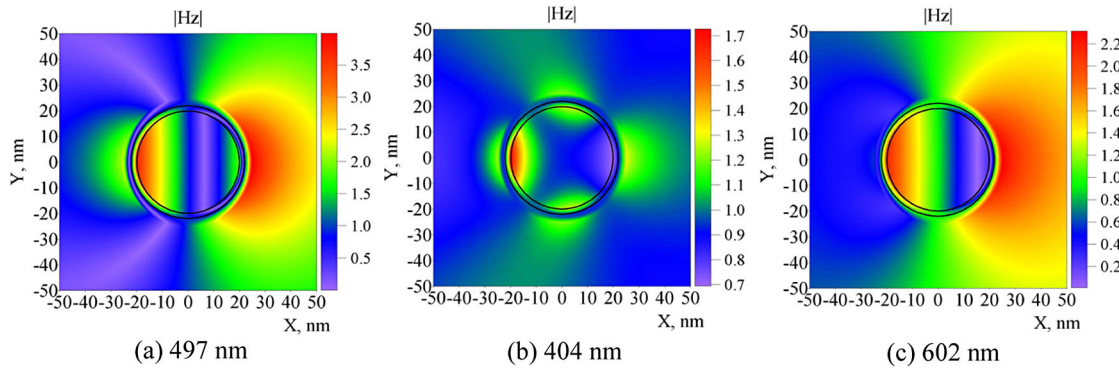
Fig. 6.   In-resonance magnetic field patterns for (a), (b) silver and (c), (d) gold nanotubes in the air with the inner radius $a = 20$ nm and the thickness $h = 5$ nm at the wavelengths of peak absorption in Figs. 2(b) and 3(b). The plane wave is incident from the right.
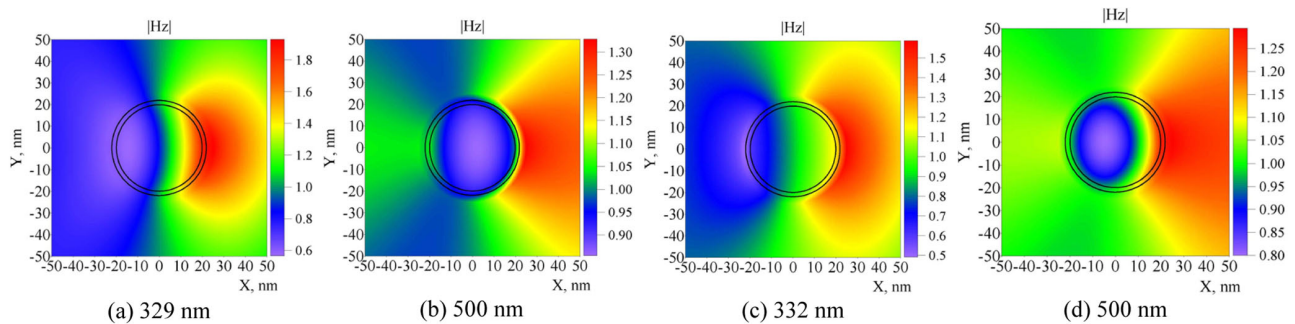
Fig. 7.   In-resonance magnetic field patterns for bimetal core–shell (a), (b) gold–silver and (c), (d) silver–gold nanowires with the core radius $a = 20$ nm and shell thickness $h = 5$ nm at the wavelengths of peak absorption in Figs. 4(b) and 5(b). The plane wave is incident from the right.

shell and its metal and additionally, but only if the shell is ultra-thin, with the core boundary and its metal. Such interpretation is in good agreement with in-resonance near-field patterns, shown in Figs. 6 and 7 for thinner-than-skin-depth shells.

The resonances explained above are in full agreement with the quasi-static characteristic Eq. (4), which is valid for arbitrary complex dielectric permittivities of the shell, ε_M, and the core, ε_{in}, and arbitrary ratio of the inner to outer tube radius. Indeed, close inspection of this equation shows that if the core material is also metal, with $\mathrm{Re}\,\varepsilon_{in} < 0$, it takes the following main-term forms in two opposite cases:

$$\mathrm{Re}\,\varepsilon_M(\lambda_m) + 1 = O(mh^2/a^2) \quad \text{if} \quad h/a \to 0, \qquad (5)$$

$$\mathrm{Re}\,\varepsilon_{in}(\lambda_m) + 1 = O(ma^2/h^2) \quad \text{if} \quad a/h \to 0. \qquad (6)$$

Of course, Eq. (4) and its limiting forms Eqs. (5) and (6) give good results only if the losses in metals can be neglected. Otherwise, one should look for the minimum of the respective function $|\varepsilon(\lambda) + 1|$ that leads to the modified equations, similar to Eq. (2).

To obtain a better understanding of the above-mentioned effects, we have also computed the maps of TSCS and ACS as functions of two parameters, namely, the wavelength and
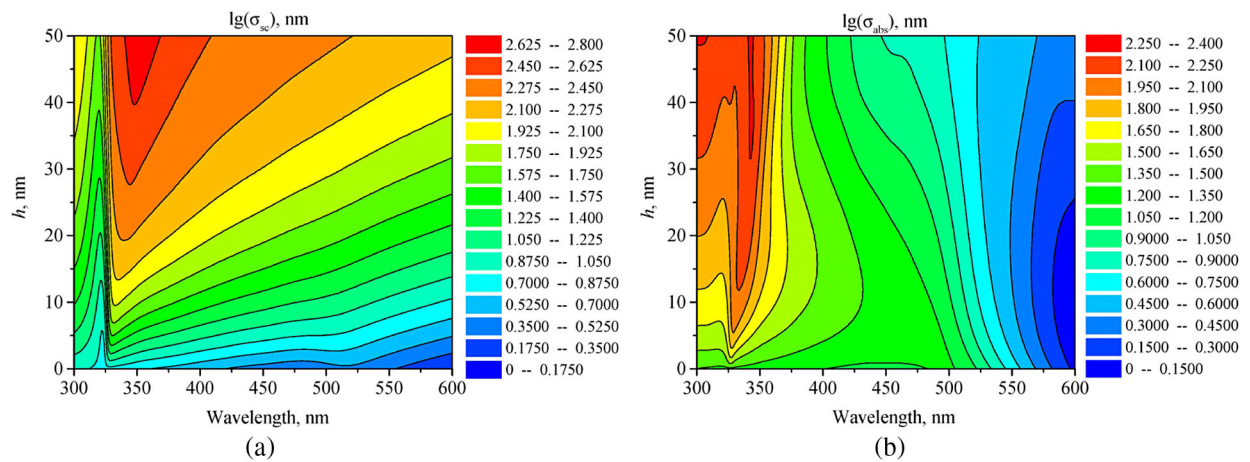
Fig. 8. Reliefs of (a) TSCS and (b) ACS as a function of the wavelength and the silver shell thickness, for bimetal wire with gold core radius $a = 20$ nm.
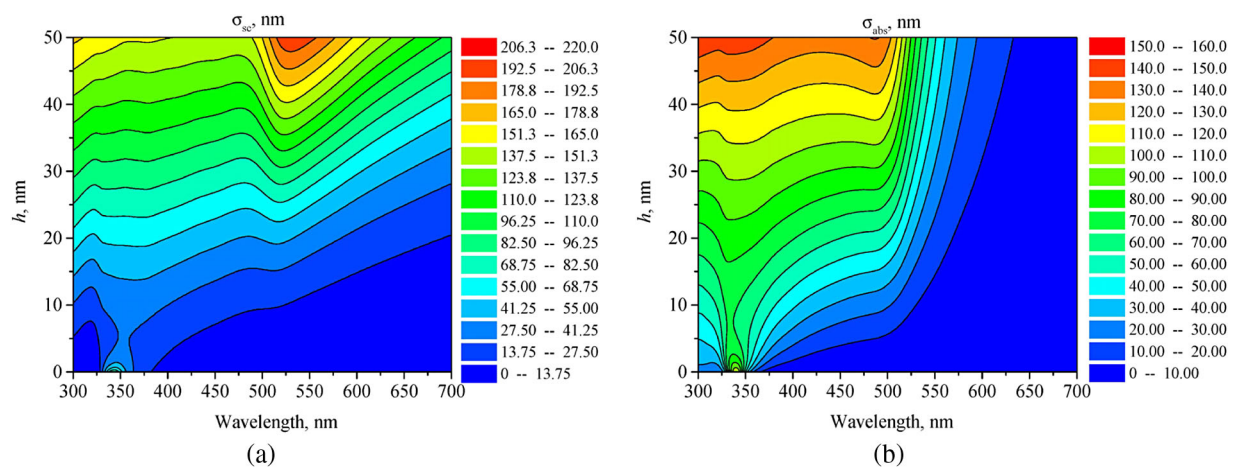
Fig. 9. Same as in Fig. 8, but for bimetal silver–gold nanowire with the silver core radius $a = 20$ nm.

the thickness of shell layer. In Fig. 8, such maps are shown for bimetal gold–silver nanowire with the core radius $a = 20$ nm, and in Fig. 9 for silver–gold nanowire. On these maps, one can see that an extremely thin silver shell on a gold wire, of some 2 nm thickness, is enough to suppress completely the LSP peak associated with gold: only the silver-wire LSP peak remains in the spectra of both the scattering and the absorption. In contrast, if a silver nanowire is coated with gold shell, then the silver LSP peak keeps dominating over the gold LSP peak until the shell thickness gets over 30 nm.

Of course, if the thickness of the tube wall is around 2 nm or smaller, then the non-local effects on the dielectric function of silver become sizable because such a thickness is comparable to the collision-free path of electrons in silver. It is known that account of non-local effects results mainly in the additional losses, i.e., in larger values of Im ε. In such a case, our results become rather upper-limit estimation.

These features of the spectral behavior of bimetal nanowires can be useful in the design of optical nanowire bio- and chemosensors of small changes in the host medium refractive index. They should be taken into account in the research into nonlinear optics including second-harmonic generation and

surface-enhanced Raman spectroscopy for rapid detection of multiple organophosphorus pesticides in foods [1].

4. SUMMARY

As we have shown, bimetal core–shell nanowires made of gold and silver display only the broad collective resonances, caused by the LSP modes (of all azimuth indices) of the shell's outer surface and, if the shell is extremely thin (thinner than the skin depth of the shell's metal), on the LSP modes of the core. These two types of modes do not hybridize between themselves. This is in contrast to the LSP modes of thin metal nanotubes in dielectric media. The reason is the "negative dielectric" nature of both metals in the visible range: the boundary between them cannot guide a surface plasmon wave. As a consequence, on finite boundaries, such as the boundary between the core and the shell of different metals, no standing wave, i.e., no LSP mode can be supported.

These observations allow one to conclude that the main effect in the resonance scattering of visible light that accompanies replacement of a single-metal nanowire with a bimetal core–shell nanowire, is combination, or overlap, of two separate

LSP resonances on solid circular wire made of each metal. This overlap is observed, however, only if the shell thickness is sufficiently small, smaller than the skin depth of the shell's metal. Such a combination can be still useful as it widens the range of bright scattering and intensive absorption to the whole interval between approximately 340 nm (circular silver-wire LSP peak) and 520 nm (circular gold-wire LSP peak). As each resonance is accompanied with a near-field enhancement, bimetal nanowires can improve the bandwidth characteristics of spectroscopic sensors used in rapid detection of harmful substances.

Disclosures.   The authors declare no conflicts of interest.

REFERENCES

1. T. Yaseen, H. Pu, and D.-W. Sun, "Rapid detection of multiple organophosphorus pesticides (triazophos and parathion-methyl) residues in peach by SERS based on core-shell bimetallic Au@Ag NPs," Food Addit. Contamin. A **36**, 762–778 (2019).

2. B. Zhang, W. Li, J. Jiu, Y. Yang, J. Jing, K. Suganuma, and C.-F. Li, "Large-scale and galvanic replacement free synthesis of Cu@Ag core–shell nanowires for flexible electronics," Inorg. Chem. **58**, 3374–3381 (2019).

3. L. Novotny and B. Hecht, *Principles of Nano-Optics*, 2nd ed. (Cambridge University, 2012).

4. E. A. Velichko and A. P. Nickolaenko, "Nanocylinders made of noble metals as scatterers of plane electromagnetic wave," Telecommun. Radio Eng. **75**, 369–381 (2016).

5. E. A. Velichko and A. I. Nosich, "Refractive-index sensitivities of hybrid surface-plasmon resonances for a core-shell circular silver nanotube sensor," Opt. Lett. **38**, 4978–4981 (2013).

6. E. A. Velichko and D. M. Natarov, "Localized versus delocalized surface plasmons: dual nature of resonances on a silver circular wire and a silver tube of large diameter," J. Opt. **20**, 075002 (2018).

7. J. Zhu, "Surface plasmon resonance from bimetallic interface in Au-Ag core-shell structure nanowires," Nano. Res. Lett. **4**, 977–981 (2009).

8. J. W. Strutt and L. Rayleigh, "On the electromagnetic theory of light," Philos. Mag. **12**(73), 81–101 (1881).

9. E. I. Smotrova, T. M. Benson, P. Sewell, J. Ctyroky, and A. I. Nosich, "Lasing frequencies and thresholds of the dipole-type supermodes in an active microdisk concentrically coupled with a passive microring," J. Opt. Soc. Am. A **25**, 2884–2892 (2008).

10. A. S. Zolotukhina, A. O. Spiridonov, E. M. Karchevskii, and A. I. Nosich, "Electromagnetic analysis of optimal pumping of a microdisk laser with a ring electrode," Appl. Phys. B **123**, 32 (2017).

11. D. M. Natarov, T. M. Benson, and A. I. Nosich, "Electromagnetic analysis of the lasing thresholds of hybrid plasmon modes of a silver tube nanolaser with active core and active shell," Beilstein J. Nanotechnol. **10**, 294–304 (2019).

12. P. B. Johnson and R. W. Christy, "Optical constants of the noble metals," Phys. Rev. B **6**, 4370–4378 (1972).